Applied and Environmental Microbiology, Apr. 2008, p. 2135–2143 Vol. 74, No. 7
0099-2240/08/$08.00+0 doi:10.1128/AEM.02304-07

Fluorescence Correlation Spectroscopy To Study Diffusion and Reaction of Bacteriophages inside Biofilms[▽]

R. Briandet,[1,5]* P. Lacroix-Gueu,[2] M. Renault,[1,5] S. Lecart,[3] T. Meylheuc,[1,5] E. Bidnenko,[4] K. Steenkeste,[2] M.-N. Bellon-Fontaine,[1,5] and M.-P. Fontaine-Aupart[2]

INRA, UMR Bioadhésion et Hygiène des Matériaux, F-91300 Massy, France[1]; Laboratoire de Photophysique Moléculaire, CNRS UPR 3361, Université Paris-Sud, F-91405 Orsay Cedex, France[2]; Centre de Photonique Biomédicale, Centre Laser de l'Université Paris-Sud, Université Paris-Sud, F-91405 Orsay Cedex, France[3]; INRA, Unité Génétique Microbienne, Domaine de Vilvert, F-78352 Jouy-en-Josas, France[4]; and AgroParisTech, UMR Bioadhésion et Hygiène des Matériaux, F-91300 Massy, France[5]

Received 11 October 2007/Accepted 25 January 2008

In the natural environment, most of the phages that target bacteria are thought to exist in biofilm ecosystems. The purpose of this study was to gain a clearer understanding of the reactivity of these viral particles when they come into contact with bacteria embedded in biofilms. Experimentally, we quantified lactococcal c2 phage diffusion and reaction through model biofilms using in situ fluorescence correlation spectroscopy with two-photon excitation. Correlation curves for fluorescently labeled c2 phage in nonreacting *Stenotrophomonas maltophilia* biofilms indicated that extracellular polymeric substances did not provide significant resistance to phage penetration and diffusion, even though penetration and diffusion were sometimes restricted because of the noncontractile tail of the viral particle. Fluctuations in the fluorescence intensity of the labeled phage were detected throughout the thickness of biofilms formed by c2-sensitive and c2-resistant strains of *Lactococcus lactis* but could never be correlated with time, revealing that the phage was immobile. This finding confirmed that recognition binding receptors for the viral particles were present on the resistant bacterial cell wall. Taken together, our results suggest that biofilms may act as "active" phage reservoirs that can entrap and amplify viral particles and protect them from harsh environments.

Bacteriophages (phages) are viruses that attack prokaryotic cells (bacteria and archaea). Phage populations are highly dynamic and represent the most diverse and abundant life forms on earth. Outside a host, phages are thought to be metabolically inert particles, incapable of performing biosynthetic functions. The phage development cycle (genome replication and synthesis of capsid components) occurs only within infected cells, via the lytic or lysogenic pathway. The lytic pathway may result in cell death, destruction of the bacterial population, and release of progeny phage particles or, in the case of filamentous phages, continuous extrusion of phages without cell death (17, 48). The lysogenic pathway results in establishment of the phage genome inside the bacterial cell, where it can remain in a dormant state for generations, replicating in synchronization with the bacterial chromosome. An important feature is the possible conversion from lysogeny to lytic development, which can occur spontaneously or be induced by various factors. Thus, the impact of phages on bacterial ecosystems and their key role in the adaptive evolution of bacteria cannot be underestimated (6, 39, 40). Accumulated data from sequence analyses indicate that up to 20% of each bacterial genome may consist of phage-related DNA (8). The importance of these phage-related sequences to bacterial evolution is more striking in the context of lysogenic conversion (e.g., when numerous bacterial toxins are encoded by converting prophages) (32). Furthermore, prophages can cause DNA inversions and phenotypic variations and can mediate cell death, which is an important differentiation mechanism within microcolonies (40, 56, 57).

Because of this biological activity, phages are of considerable biotechnological interest (e.g., due to their antimicrobial activity) in the fields of health and agriculture (1, 26). The emergence of pathogenic bacteria resistant to antimicrobial agents has highlighted the need for alternative means to treat human and animal bacterial infections. In this context, there are new prospects for phage therapy in the form of the application or ingestion of phage particles as an alternative to antibiotics (1, 11, 14, 21, 32, 35, 41, 48, 51). A recent major breakthrough for phage therapy was the approval by the U.S. Food and Drug Administration of a cocktail of bacteriophages as a treatment for *Listeria monocytogenes* contamination in ready-to-eat meat and poultry products (5). This approval may open the way for other applications (21).

On the other hand, bacteriophages can be substantial problems in the food industry. Most research on the control of problematic phages has been carried out in the dairy industry (7, 34). At present, industrial milk fermentation using lactic acid bacteria is prone to bacteriophage attack because of the routine presence of different lytic bacteriophage groups in the environment. Following phage infection, the starter culture is rapidly lysed, causing a drastic reduction in the rate of milk acidification and thus major financial losses and high economic cost (20).

Thus, one question is how such phage activity can occur. To answer this question, it is necessary to understand that most

* Corresponding author. Mailing address: UMR763 BHM INRA-AgroParisTech, 25 Avenue République, 91300 Massy, France. Phone: 33 (0)1 69 53 64 77. Fax: 33 (0)1 69 93 51 44. E-mail: romain.briandet@jouy.inra.fr.

▽ Published ahead of print on 1 February 2008.

phages that target bacteria in natural environments are thought to exist in biofilm ecosystems. The reciprocal effects of biofilm structure and the activity of the prophages released have previously been demonstrated for different bacterial species (25, 44, 57). However, the reaction of biofilms to ubiquitous viral particles in the environment is poorly documented (52). It is clearly essential to determine whether a bacteriophage can directly penetrate the glycocalix matrix, infect the bacteria, and ultimately degrade biofilms (27, 28), as these fundamental ecological questions must be answered if we are to improve phage control.

Although phages have been proposed as a way to destroy or control biofilms, the necessary technology has not been developed yet to a sufficient degree. At an early stage, we reported successful application of fluorescence correlation spectroscopy (FCS) to analysis of molecular mobility and/or the inhibition of mobility of fluorescently labeled nanoprobes diffusing within bacterial biofilms (24). Indeed, this method has now become an ultrasensitive technique for monitoring molecular dynamics operating at the single-molecule level (46). The movement of fluorescent molecules through a microvolume generates temporal fluctuations in the emitted fluorescence. Analysis of the autocorrelation of these fluctuations may provide different parameters and, in particular, the translational diffusion coefficients of fluorescent probes with submicrometer resolution. Thanks to the inherent averaging of thousands of single-molecule diffusion events, FCS determines diffusion coefficients in short acquisition times (usually tens of seconds) and with statistical confidence. Furthermore, due to the very weak concentration of fluorophores used and the small volume probed, FCS is well suited to confocal microscopy and enables noninvasive in vivo studies by comparison with fluorescence recovery after photobleaching, which can generate perturbations in a biological system (38). Since the introduction of two-photon excitation (TPE), FCS combined with TPE has several advantages. The principle of TPE is the simultaneous absorption of two photons with one-half the energy needed for a one-photon transition. The probability of this phenomenon is very small and thus confines the excitation to the objective focal point, the region where the temporal and spatial concentrations of photons are very high. This inherent optical sectioning enables studies in femtoliter volumes with very low background. Moreover, since the absorption is limited to the focal region, photobleaching and photodamage are restricted to the excitation volume.

This paper describes the application of FCS with TPE to investigation of the different effects of phages on biofilm components (diffusion through the biomass and/or reaction with host bacteria). This was accomplished using a model dairy bacteriophage, c2, specific for *Lactococcus lactis* subsp. *cremoris* in (i) biofilms of two lactococcal strains, *Lactococcus lactis* subsp. *cremoris* OSM31 (the natural host of phage c2) and *Lactococcus lactis* subsp. *lactis* IL-1403 (the facultative host of phage c2), and (ii) biofilms of the c2-resistant organism *Stenotrophomonas maltophilia*, a spoilage bacterium frequently isolated from surfaces in dairy plants.

MATERIALS AND METHODS

Biological materials. (i) Bacterial strains and culture conditions. Three bacterial strains were used in this study, *Stenotrophomonas maltophilia* 114N-Sm (referred to in the text as *S. maltophilia*) (30) (a gram-negative spoilage bacterium isolated from a surface in a dairy plant), *Lactococcus lactis* subsp. *lactis* IL-1403 (3), and *Lactococcus lactis* subsp. *cremoris* OSM31 (kindly provided by M. Y. Mistou, INRA, Jouy-en-Josas, France). Stock cultures were prepared by mixing stationary-phase cultures with a 40% (vol/vol) glycerol solution. After two subcultures, *S. maltophilia* 114N-Sm was cultivated overnight at 30°C in Trypticase soy broth (bioMérieux, France), while both *L. lactis* strains were cultivated overnight in M17 broth (BD-Difco, France) supplemented with 0.5% glucose at 30°C. To obtain biofilm formation in continuous-flow cells, bacterial cultures were washed using three centrifugation steps (7,000 × *g*, 4°C, 10 min) and resuspended in 150 mM NaCl. The bacterial concentration was adjusted to 10^8 CFU/ml by adjusting the absorbance at 400 nm. Two milliliters of a suspension was poured into a parallel flow cell (BST FC81; Biosurface Technology, Bozeman, MT) using a sterile syringe. After 3 h of static adhesion on the bottom glass coverslip in 150 mM NaCl, growth medium at a continuous flow rate of 0.5 ml · min^{-1} was circulated with a peristaltic pump (model 205S; Watson and Marlow, Dreux, France) at 30°C over a 24-h period.

(ii) Prolate bacteriophage. The model viral particle used during this study was a c2 lactococcal phage. The 22,163-bp genome of this bacteriophage has been fully sequenced (34). This c2 phage exhibits a prolate structure with a ~100-nm-diameter head and a ~150- to 200-nm noncontractile tail, as determined by scanning electron microscopy (SEM) (34). The c2 phage was kindly provided by S. Kulakauskas (INRA UBLO, Jouy-en-Josas, France) and was stored at 4°C in 150 mM NaCl. Phage titration was performed when necessary using the serial dilution technique and formation of lytic plaques on a layer of sensitive bacteria in a petri dish, as described previously (53). Briefly, 0.1 ml of a phage suspension was added to 0.2 ml of a mid-log-phase bacterial culture of the sensitive bacterium *L. lactis*. Then 30 μl of 1 M $CaCl_2$ was added to encourage phage infection, and the coculture was incubated for 10 min at 30°C. Each coculture was added to 3 ml of soft agar (M17 [BD-Difco] supplemented with 8 g/liter agar and 0.5% sucrose) in order to create a soft double layer on agar plates (M17 [Oxoid] supplemented with 11 g/liter agar and 0.5% sucrose). The petri dishes were incubated overnight at 30°C in order to enumerate the visible lytic plaques.

For phage amplification, 10^8 PFU of the c2 phage was added to 400 ml of a sensitive *L. lactis* culture (optical density at 600 nm, 0.1). Infected bacterial cells were incubated at 30°C until clearance of the suspension was observed. The coculture was then centrifuged for 10 min at 7,000 × *g* and 4°C to eliminate bacterial debris. Phage particles were then washed with 150 mM NaCl by centrifugation at 18,000 × *g* for 6 h. The pellet was resuspended in 10 ml of 150 mM NaCl and sterilized by filtration (0.22 μm; Steriflip; Millipore). The final phage suspension, containing 10^{10} PFU/ml, was stored at 4°C.

Microscopic observation of the biofilm architecture. Direct in situ observation of biofilms in flow cells was performed with a Leica SP2 AOBS confocal spectral microscope (CLSM) (Leica Microsystems, France) at the MIMA2 microscopy platform (http://voxel.jouy.inra.fr/mima2). Bacteria from the biofilms were stained with 2 ml of 5 μM Syto 61 nucleic acid dye (Molecular Probes) that was aseptically injected into the flow cell with a syringe. After 10 min, the flow cell was mounted under the ×40 objective of the microscope (numerical aperture, 1.2). Bonded Syto 61 molecules were excited at 633 nm with a HeNe laser beam, and fluorescence was collected with a photomultiplier in the range from 650 to 700 nm.

Ex situ high-magnification imaging of the biofilms was performed by scanning electron microscopy (SEM) (S-4500; Hitachi, Tokyo, Japan) at the MIMA2 microscopy platform. To prevent biofilm dispersal, all chemical preparation of the samples was carried out directly in the flow cell used to grow the biofilms. Each sample was fixed with 3% glutaraldehyde for 1 h at 4°C and washed three times with sodium cacodylate (0.2 M, pH 7.4). The fixed cells were then washed with sodium cacodylate and dehydrated by passage through a graded series of ethanol-water solutions containing 70% ethanol (three times for 15 min each), 90% ethanol (three times for 15 min each), 95% ethanol (three times for 15 min each), and 100% ethanol (three times for 15 min each). The samples were then kept desiccated before gold sputtering and viewing (10 kV) with the SEM.

Fluorescent nanoprobes. Anionic carboxylate-modified fluorescent latex beads of 110 nm in diameter (Molecular Probes) were used as a reference. The beads were suspended in deionized water (Purit, France). The suspensions were filtered and sonicated prior to each experiment in order to eliminate most of the aggregates. The final concentrations ranged from 1 nM (in solution) to 10 nM (in biofilms).

The following selection criteria for bacteriophage fluorescent labeling were imposed by the experimental conditions required for FCS with TPE (see below) and the properties of the biological entities: (i) the fluorophore had to be excited by two photons in the wavelength range from 700 to 900 nm; (ii) detection of the fluorescence signal emitted during the counting interval had to be significant

despite the low excitation energy and low fluorophore concentration employed, necessitating the use of a fluorophore with a significant fluorescence quantum yield; and (iii) the fluorophore had to be able to label the bacteriophage and not living cells inside the biofilms. In the light of these requirements, the fluorescent dye Sytox green (from Molecular Probes) was chosen. Only dead bacteria in biofilms (less than 10%) can be stained by this fluorophore. The control of bacteriophage staining is described in the Results.

The following procedure was used to stain the bacteriophage. Ten milliliters of a c2 suspension titrated to obtain 10^{10} PFU/ml in 150 mM NaCl was mixed with 100 μl of Sytox green (5 mM) and incubated at room temperature (24°C) for 2 h under agitation. The excess free fluorophore was removed by careful rinsing. The labeled bacteriophage suspension was used unchanged for FCS measurements in biofilms and was diluted 10-fold for experiments in solution.

Before FCS measurement inside biofilms, the growth medium flow was stopped and 2 ml of the target fluorophore (reference latex beads or Sytox green-labeled phage) was aseptically injected into the flow cell.

Stationary spectroscopy. The absorption and fluorescence steady-state spectra were measured using a Cary 300 double-beam UV-visible spectrophotometer (Varian) and a Perkin Elmer MPF-3L spectrofluorimeter, respectively. For fluorescence experiments, the spectral bandwidth was adjusted to 3 nm, and the absorbance was less than 0.1 at the excitation wavelength.

Two-photon fluorescence correlation setup. The TPE correlation setup used in this study has been described in detail elsewhere (23). Briefly, it consisted of a commercial femtosecond Ti:Sapphire laser (MIRA 900 from Coherent Inc., Santa Clara, CA) (pulse duration, 100 fs; repetition rate, 76 MHz; tunable between 690 and 930 nm; average power output, ~700 mW), pumped by a continuous-wave diode-pumped solid-state laser (VERDI; Coherent Inc.). The laser beam entered a Zeiss Axiovert 135 microscope via an epifluorescence light path and was focused in the sample by an oil immersion objective (Zeiss Plan apochromat; ×63; numerical aperture, 1.4). The excitation volume defined at the focus point of our objective was estimated to be ~1.5 μm^3, corresponding to a ~500-nm beam waist and a focal depth of ~1.6 μm. Fluorescence emissions were collected through the same objective and separated from the excitation radiation by a dichroic mirror. They were then filtered through short-pass filters to absorb any diffused excitation infrared light and focused on the surface of a photomultiplier tube (R7205-01; Hamamatsu). This device was connected to a discriminator (TC 454; Oxford Instruments Inc., Oxford, United Kingdom), and the signal output was transmitted to a digital autocorrelator module (Flex2kx2-12 correlator), which computed online the correlation function of fluorescence fluctuations. To measure the translational diffusion time with 10 to 20% accuracy, the data recording times were varied from 60 s (15 iterations) to 300 s (3 iterations) for both solution and biofilm acquisitions. The data were analyzed using a routine written in-house which enabled (i) selection and averaging of chosen successive acquisitions, (ii) adaptation of different diffusion models to analyze the autocorrelation function, and (iii) calculation of associated standard deviations.

An excitation wavelength of 890 nm was used for all of the TPE experiments described here. The incident laser energy was attenuated to less than 1 mW at the sample in order to reduce the risk of photobleaching both the fluorophores and the autofluorescence signal from bacteria. Under these conditions, no cell degradation was observed during the experimental period, as verified by confocal microscopy using a live/dead bacterial viability kit (Molecular Probes).

FCS diffusion analysis. The conceptual and theoretical bases for FCS applied to molecular diffusion have been well established for several years (19). Assuming that the excitation intensity profile could be approximated using a three-dimensional Gaussian distribution and that no "blinking" dynamics of the fluorophore occurred other than its diffusion through the excitation volume, fluorescence correlation curves [$g(\tau)$] for the free Brownian motion of molecules could be fitted using the following normalized autocorrelation function:

$$g(\tau) = 1 + \left[\frac{1}{\sqrt{8}\cdot N}\right]\cdot\left[\frac{1}{1+(\tau/\tau_D)}\right]\cdot\left[\frac{1}{1+(\omega_0/z_0)^2\cdot(\tau/\tau_D)}\right]^{1/2} \quad (1)$$

where N is the mean number of fluorescent molecules in the excitation volume, z_0 is the axial dimension of the detection volume, ω_0 is the lateral dimension of the detection volume, τ is the temporal gate of photon acquisition, and τ_D is the translational diffusion time. It should be noted that FCS measurements require low N values to be detected and thus allow access to single-molecule detection (4). z_0 and ω_0 are recovered by fitting the measured correlation curve to 50-nm-radius spheres diffusing in water (with a diffusion value given by the Stokes-Einstein relation, $D = 4\ \mu m^2\cdot s^{-1}$, where D is the diffusion coefficient with biphotonic excitation). We were thus able to determine that ω_0/z_0 is 0.30 ± 0.03 (23), which was then used for all other measurements. D could be related to τ_D using the equation:

$$D = \omega_0^2/8\tau_D \quad (2)$$

When two different populations could diffuse in a medium, the autocorrelation function had to be rewritten as follows:

$$g(\tau) = 1 + \frac{1}{\sqrt{8N}}\left\{a\left[\frac{1}{1+(\tau/\tau_1)}\right]\left[\frac{1}{1+(\omega_0/z_0)^2(\tau/\tau_1)}\right]^{1/2} + (1-a)\left[\frac{1}{1+(\tau/\tau_2)}\right]\left[\frac{1}{1+(\omega_0/z_0)^2(\tau/\tau_2)}\right]^{1/2}\right\} \quad (3)$$

where α and 1 − α are the fractions of the molar concentrations of the two diffusive species and τ_1 and τ_2 are their respective translational diffusion times. During the experiments described below, all fluorescence curves could be fitted satisfactorily using a one- or two-component model. Thus, the anomalous diffusion which might occur in a complex biological environment (55) was not considered.

RESULTS

Microscopic observations of the architecture of bacterial biofilms. In order to gain a clearer understanding of the model biofilms studied, we examined their three-dimensional structure using SEM (Fig. 1) and in situ CLSM (Fig. 2). These two microscopic techniques are complementary because biofilms observed with confocal microscopy are fully hydrated but limited by the optical resolution (submicrometer), while SEM generates high-resolution (nanometer) images but requires dehydration of samples prior to metallization and observation.

The *L. lactis* biofilm structures revealed by SEM comprised a regular assembly of cells with no voids between the bacteria (Fig. 1a and 1b). The high resolution of our SEM images made it possible to identify the replication septa of individual cells within the biofilms and some residual extracellular polymeric substances (EPS) between the bacteria (Fig. 1b). The existence of an EPS matrix, contrary to previous hypotheses (16), was confirmed by in situ observations using CLSM. Figure 2a shows a loosened structure in which the bacteria were quasi-monodispersed and embedded in a continuous extracellular matrix that held the cells in position.

By contrast, the structure of 24-h *S. maltophilia* biofilms was markedly heterogeneous, as shown by both SEM and CLSM (Fig. 1c, 1d, and 2b). These biofilms consisted of a basal layer of bacterial cells with patchy, three-dimensional compact aggregates that could be compared to the "mushroom-like" structure frequently described for other gram-negative strains (29, 31). This structure was attributed to the presence of an organic extracellular matrix composed of EPS, which is shown in Fig. 2b. The similar three-dimensional architectures of these biofilms in both the hydrated and dehydrated states revealed the considerable compactness of the aggregates.

Sensitivity of planktonic and biofilm cells to the c2 bacteriophage. The sensitivity of biofilm and planktonic *S. maltophilia* cells or *L. lactis* OSM31 and IL-1403 cells to treatment with the c2 phage was examined as described above (see Materials and Methods). Figure 3 shows the percentages of cell survival after 3 and 7 h of phage infection. As expected, the c2 phage exhibited no lytic activity toward *S. maltophilia* and *L. lactis* IL-1403 cells in either the planktonic or biofilm state. However, the phage c2 was very active against free-floating cells of *L. lactis* OMS31 (fewer than 1% of the cells survived after 7 h of infection) and to a lesser

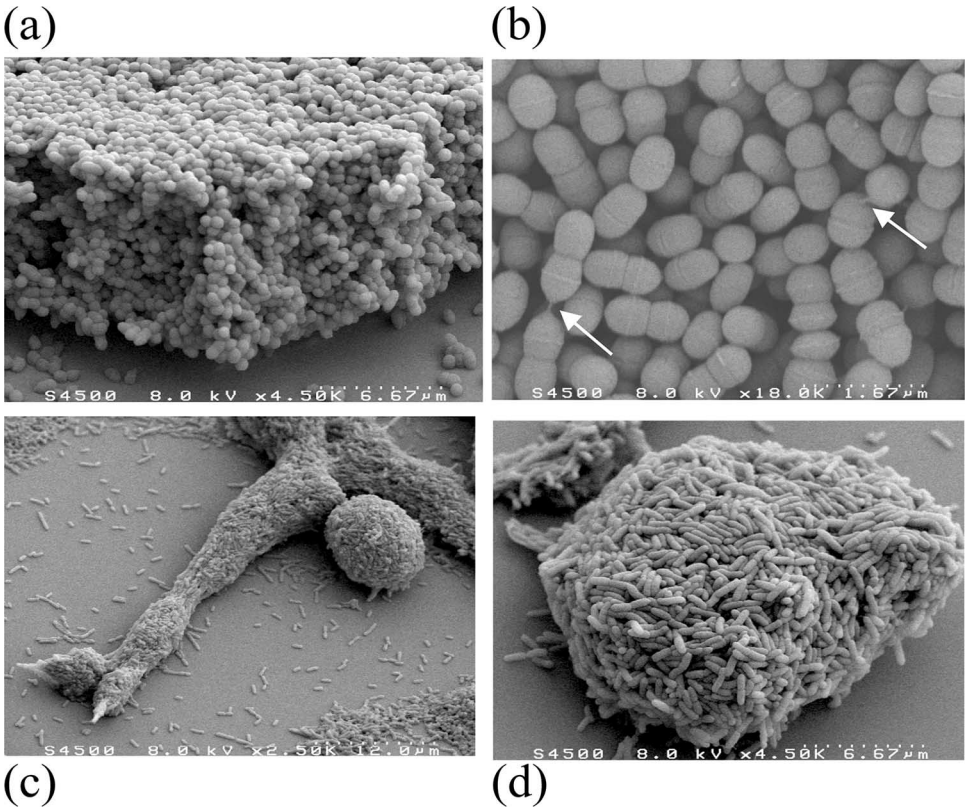

FIG. 1. SEM images of *L. lactis* OSM31 (a and b) and *S. maltophilia* (c and d) biofilms grown for 24 h at 30°C in a flow cell. The arrows in panel b indicate EPS between the bacteria.

extent against cells embedded in a biofilm structure (fewer than 25% of the cells survived after 7 h of infection). These results highlighted the increased resistance of sessile cells to phage attack compared with their planktonic counterparts, as reported previously for many of the other types of stress exerted on biofilms (dehydration, antibiotics, chemical biocides, etc.) (10, 12, 13, 15, 49). They also suggested that the location and arrangement of the biofilm substratum cell matrix could partially mask phage receptor sites (18, 27, 28).

Fluorescent labeling of c2 bacteriophage. The fluorescent nucleic acid dye Sytox green is widely employed as an indicator of viability of bacterial and eukaryotic cells (45). To our knowledge, no data have been published yet on the complexation of Sytox green with phages. We investigated this possibility by combined steady-state absorption, fluorescence spectroscopy, and FCS measurements.

Figure 4 shows the absorption and fluorescence spectra of

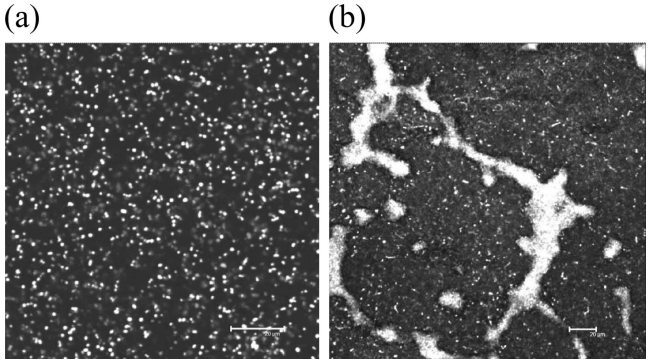

FIG. 2. CLSM images of *L. lactis* OSM31 (a) and *S. maltophilia* (b) biofilms ~5 μm from the biofilm coverslip interface. Bacterial cells were stained with the DNA-binding Syto 61 fluorophore. Bars = 20 μm.

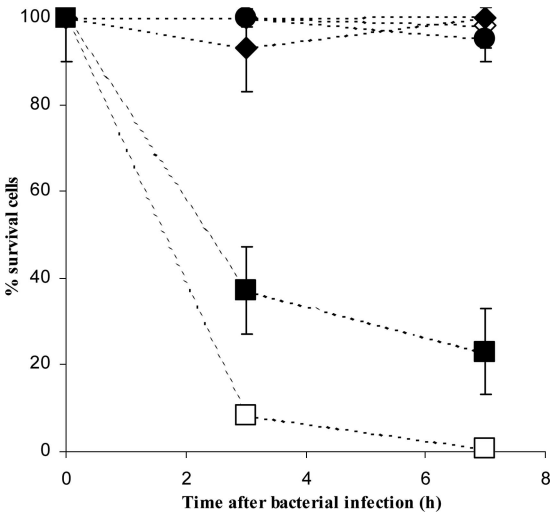

FIG. 3. Percentage of surviving bacterial cells as a function of time after c2 phage attack for strains *L. lactis* OSM31(squares), *L. lactis* IL-1403 (diamonds), and *S. maltophilia* (circles) cultivated as free cells (open symbols) or in biofilms (filled symbols). The standard deviations indicated by error bars were calculated from three independent experiments.

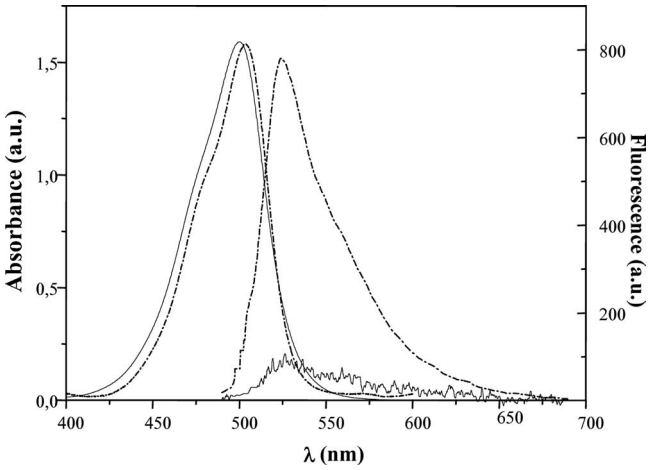

FIG. 4. Absorption and fluorescence spectra in 150 mM NaCl (pH 7.0) of free Sytox green (solid lines) and of the stain in the presence of phage (dashed and dotted lines). The fluorescence spectra were obtained with excitation at 500 nm and with the same absorbance (0.1 absorbance unit [a.u.]) for both free Sytox green and Sytox green-stained phages.

Sytox green in the presence of c2 particles, together with the corresponding spectra of the free fluorophore as a control. The changes in the absorption spectra induced by the presence of phage corresponded to a 4-nm red shift of the maximum (from 500 to 504 nm) and the appearance of an isobestic point at 520 nm, both of which suggested the formation of a Sytox green-phage complex. The shapes of the fluorescence spectra for Sytox green in the absence and presence of phage were almost indistinguishable, with a maximum at 525 nm as reported previously (45), but a ~10-fold increase in fluorescence was observed in the presence of phage. These findings confirmed the penetration of Sytox green into phage particles and clarified its interaction with phage DNA.

This Sytox green-phage complexation was confirmed by FCS measurements. Figure 5 shows the correlation curve obtained for stained phage by comparison with free Sytox green in solution. Using the Brownian diffusion model (equation 1), the diffusion coefficient of free Sytox green was calculated to be ~270 $\mu m^2 \cdot s^{-1}$, corresponding to a diffusion lifetime of ~120 μs. Thus, assuming that the molecule is spherical, the radius of Sytox green was estimated to be ~1 nm, which is in agreement with the radius of the chromophores (2). For stained phage, the correlation curve was well fitted by a two-component model (equation 2), as shown in Fig. 5. An initial diffusion lifetime (τ_1) of 12.0 ± 2 ms ($D = 2.7\ \mu m^2 \cdot s^{-1}$) was obtained and could reasonably be assigned to the diffusion of Sytox green associated with monomeric phage (as a control, we verified that unstained phage did not generate any FCS signal). In addition, the τ_2 value obtained by fitting the correlation curves with equation 2 for stained c2 phage in aqueous biofilms was 74 ± 10 ms, and the corresponding α_1 and α_2 values were 62% ± 6% and 38% ± 5%, respectively. The τ_1 value was only 1.5-fold

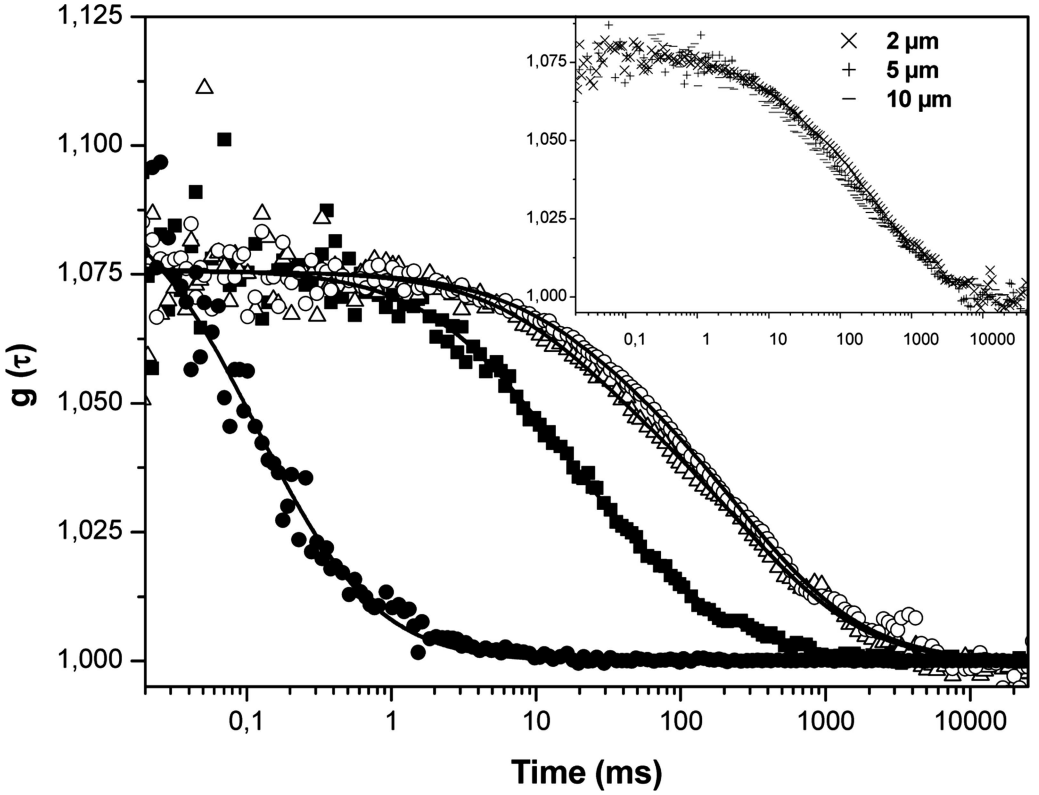

FIG. 5. g(τ) for c2 bacteriophage stained with Sytox green in solution (■) and in homogeneous (△) and heterogeneous (○) zones of *S. maltophilia* biofilms. The fit of the curves (straight lines) was obtained using equation 2. For comparison, the fluorescence correlation curve for free Sytox green in solution (●) is also shown (fit obtained using equation 1). (Inset) Fluorescence correlation curves obtained at different depths from the biofilm coverslip interface in a heterogeneous zone of a biofilm. The numbers of particles in the excitation volume were ~ 10 in solution and ~30 to 50 in biofilms.

higher for the bacteriophage than for monomeric fluorescent latex beads with a diameter of 110 nm (the size of a bacteriophage head) (8.2 ± 0.7 ms), which was in line with the influence of the virus tail in terms of its mobility. Also, the τ_2 value for the fluorescent latex beads was 50 ± 10 ms, and the corresponding α_1 and α_2 values were 84 ± 6% and 16% ± 6%, respectively. The diffusion lifetime of stained bacteriophage aggregates (~40%) was five- to sevenfold higher than that of the monomeric phage (τ_2 = 74 ± 11 ms). Based on these data, the corresponding average diffusion time for stained bacteriophage was estimated to be 26 ms, a result similar to that obtained using a single diffusing species (30).

The data presented here show that Sytox green could be used for efficient labeling of bacteriophage particles.

FCS measurement of bacteriophage diffusion in situ. The diffusion of c2 phage within bacterial biofilms was first examined using biofilms formed by *S. maltophilia* bacteria. The high degree of specific recognition between lactococcal phage and their target site precluded any specific binding to these bacteria. Furthermore, the occurrence of electrostatic interactions which might influence phage retention within biofilms could also be reasonably excluded because electrophoretic mobility measurements revealed a global negative charge for the surfaces of both phage and bacteria (data not shown). Observation of c2 phage mobility could therefore be expected.

Autocorrelation functions for the diffusion of Sytox green-labeled c2 phage were measured in various parts of the biofilm, including rich EPS areas and different depths (Fig. 5). The corresponding correlation curves were found to be best described by a model with only two different populations found at similar proportions in both solution and biofilm. However, the curve profiles for stained bacteriophage in biofilms differed markedly from the curve profiles for stained bacteriophage in pure water, and the distortions increased only with the compactness of the local biofilm structure (Fig. 5). Using a two-diffusing-species model (equation 2), the fit of experimental data was clear at all points within the biofilm (Fig. 5), and relatively reproducible values were obtained. In the homogeneous zone of *S. maltophilia* biofilms, the τ_1 and τ_2 values were 27 ± 3 and 345 ± 110 ms, respectively, and the α_1 and α_2 values were 70% ± 10% and 30% ± 5%, respectively; in the heterogeneous zone the τ_1 and τ_2 values were 22 ± 3 and 540 ± 200, respectively, and the α_1 and α_2 values were 60% ± 6% and 40% ± 5%, respectively. Thus, we found that τ_1 was ~25 ms, corresponding to a diffusion coefficient of ~1.3 $\mu m^2 \cdot s^{-1}$, a value twofold lower than the value obtained with pure water. This could be attributed to different local viscosity changes in water and in the biofilm. To verify this hypothesis, we compared the mobilities of reference latex beads in these environments. Indeed, applying the Stoke-Einstein equation to spherical nanoparticles with a hydrodynamic radius *R*, local viscosity (η) could be linked to the translational diffusion time (τ) (obtained by FCS measurement) using the equation:

$$\eta = 4kT\tau/3\pi R\omega_0^2 \quad (4)$$

where ω_0 is the beam waist at the focal point. We determined that monomeric latex beads diffused in the biofilm (Fig. 6) with a τ value of 13 ± 2 ms, which corresponded to a local viscosity of ~1.5 cP (equation 4). This result revealed that the EPS

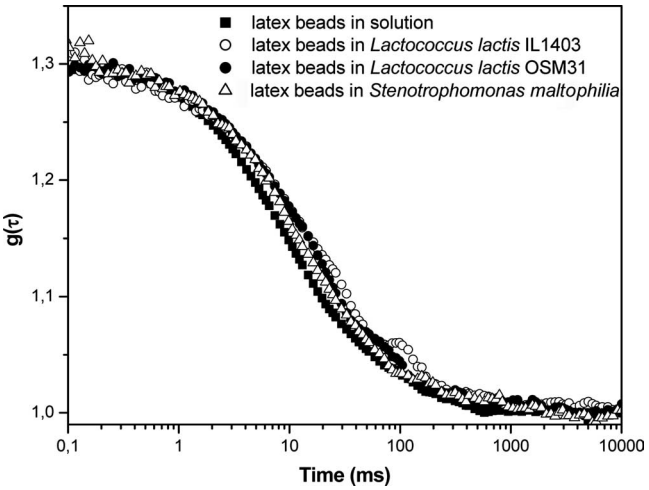

FIG. 6. Shift of fluorescence correlation curves for anionic fluorescent latex beads (radius, 55 nm) in solution and at various points on the same plane of the three biofilms studied. Curve fitting was accomplished using equation 2. The numbers of particles in the excitation volume were ~1 in solution and ~5 to 10 in biofilms.

matrix of the biofilm was slightly more viscous than water (η_{water} = 0.96 cP), thus highlighting the influence of viscosity on mass transfer. By comparison, the ratio of the τ_1 diffusion lifetime of c2 phage in water to the τ_1 diffusion lifetime of c2 phage in a biofilm reached ~2.2, emphasizing the role of c2 phage morphology in the diffusion process.

This factor was clearly observed with respect to τ_2 values (see above), which could vary considerably within a *S. maltophilia* biofilm, depending on the location selected (homogeneous or heterogeneous zone). Furthermore, these τ_2 values were higher than those obtained for latex beads, revealing that the behavior of viral particles was more complex, as discussed below.

c2 phage diffusion within the two *L. lactis* biofilms was also studied. The τ_1 and τ_2 values for fluorescent latex beads in all parts of *L. lactis* biofilms were 11.4 ± 0.8 and 70 ± 15 ms, respectively, and the α_1 and α_2 values were 67% ± 10% and 33% ± 10%, respectively. No fluorescence correlation curve was obtained for c2 phage in the biofilm formed by c2-sensitive *L. lactis* OSM31 and IL-1403 cells, which are resistant to c2 infection. However, fluorescence count rate bursts were observed if the focal laser spot was moved within the thickness and on the surface of each type of biofilm, revealing the penetration of phage particles through the biomass (Fig. 7b). In order to test whether the inhibition of diffusion of c2 particles through *L. lactis* biofilms could be attributed to their instability, FCS experiments were extended to include reference fluorescent anionic latex beads. Figure 7a shows the typical fluorescence fluctuations, and Fig. 6 shows the associated correlation curves obtained during several horizontal scans and at different depths within the biofilm. The curve was only slightly distorted compared with the curve obtained with an aqueous solution; the ratio of the diffusion coefficient for latex beads in water to the diffusion coefficient for latex beads in the biofilm was ~1.4, in good agreement when allowance was made for the estimated viscosity changes in biofilms compared with water (see above). These FCS measurements revealed

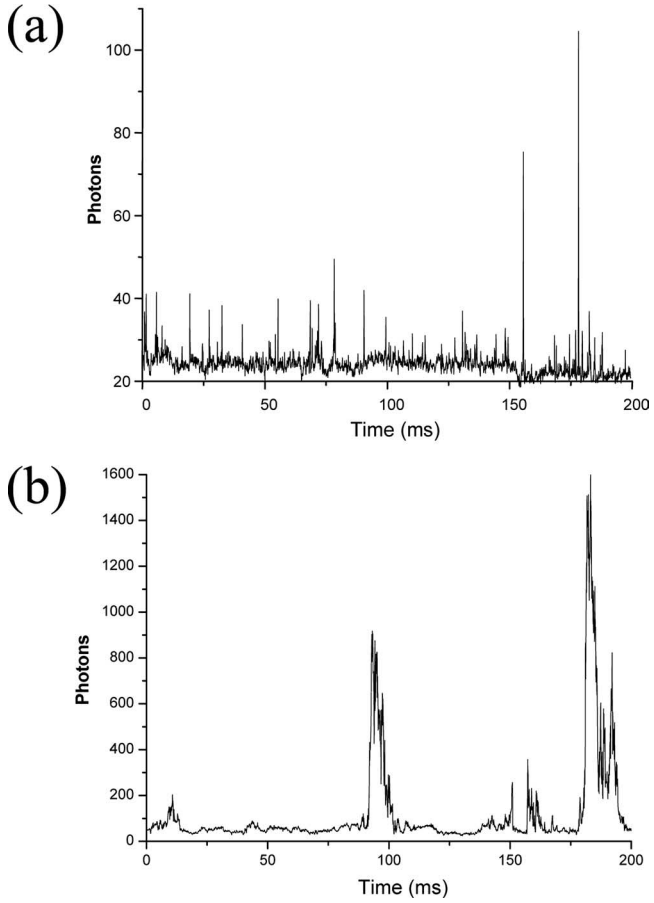

FIG. 7. (a) Typical fluorescence count rate bursts recorded for fluorescent latex beads diffusing through an *L. lactis* OSM31 biofilm. The time tracing, subjected to the autocorrelation algorithm, yielded a correlation curve $g(\tau)$ shown in Fig. 6. (b) Sytox green-stained phage diffused through the detection volume, producing a fluctuating fluorescence signal, but in this case the tracing could not be correlated over time.

that c2 phage penetrated the biofilm matrix of both *L. lactis* strains studied but were then rapidly immobilized.

DISCUSSION

The purpose of this study was to contribute to a clearer understanding of the diffusion and reaction of phages when they come into contact with bacteria embedded in biofilms. The role of the EPS matrix was studied using *S. maltophilia* biofilms composed of bacteria that are not sensitive to lactococcal c2 phage, while the access of viral particles to the surface of their host cells was examined using model *L. lactis* biofilms. As mentioned in the Introduction, and because no methodological tools have been available, very few studies have considered the diffusion and reaction of viral particles as a function of the local structure and receptor specificity of biofilms. This work demonstrated that FCS with TPE is a nondestructive and appropriate technique to study these phenomena.

Phage particle diffusion into nonreacting biofilms. The use of SEM and CLSM demonstrated the microheterogeneity of *S. maltophilia* biofilms with variable distributions of cells and EPS, as well as water-filled channels which provide phage access to the interior of biofilms. This was in agreement with the record of fluorescence correlation curves relative to the diffusion of c2 bacteriophage in all parts of the biofilm. However, these curves were dependent on biofilm structure and could never be overlaid with those obtained with water.

The analysis of FCS curves highlighted the influence of differences in viscosity between the bulk of the biofilm and water (from 0.96 to 1.5 cP) on bacteriophage diffusion. But the more important factor controlling this process is the combined role of the structures of the c2 prolate particle and the *S. maltophilia* biofilm matrix. The decrease in monomeric phage diffusion compared with that of reference latex beads could only be related to c2 phage morphology and particularly to the long, rigid tail, which could be considered the limiting factor of free mobility. But the significant increase in the diffusion lifetime values and the dispersion of phage aggregates in the heterogeneous zones of the biofilm compared to the homogeneous zones highlighted the effect of local EPS matrix compactness on the diffusion of such aggregates.

It has previously been hypothesized that EPS may protect biofilms from phage penetration (52). The most important result of our study is that *S. maltophilia* biofilms did not confer resistance to the entrapment of virus-size particles and to their diffusion even though their mobility was sometimes locally restricted. Thus, biofilms may provide a potential reservoir for such pathogens. This is consistent with previous studies that reported the persistence of enteric virions or poliovirus 1 in microbial biofilms (42, 50). Within the polymeric matrix, the virus can take advantage of the specific biofilm "lifestyle" and, in particular, can benefit from protection against environmental stress, such as desiccation or the action of antimicrobial agents (12).

Bacteriophage in reacting biofilms. As reported for antimicrobial molecules, phage was less reactive with bacteria embedded in biofilms than with free cells. The survival rate in an *L. lactis* OSM31 biofilm is in line with the data obtained for *Pseudomonas fluorescens* biofilms by Sillankorva et al. (47). To explain this result, it was hypothesized that biofilm structures may impede the access of viral particles to host bacterial cells (52). The fluorescence intensity vectors measured throughout the thickness of an *L. lactis* biofilm revealed that bacteriophage was not confined to the biofilm surface but could diffuse though the biomass; the EPS matrix did not restrict the penetration of viral particles. Probably, and as previously suggested (44), the dead cells resulting from phage attack constituted a nutrient reservoir for neighboring, surviving bacteria, thus compensating for cell starvation.

Our results confirm the significant efficiency of phage infection and subsequent lysis of bacteria in biofilms; their structure may only delay the death of biofilms in a harsh environment.

These findings supported the potential for phage therapy as an alternative to chemical antimicrobial agents (21, 35, 39, 48, 51). Such therapy would also be valuable in the context of emerging bacterial antibiotic resistance in both human therapeutics and agriculture.

Promising results have recently been obtained in studies to improve phage therapy performance (33). Novel "synthetic" biology technologies should enable the engineering of libraries

of phages with biofilm-degrading enzymes mimicking natural polysaccharases or polysaccharide lyases (27, 28, 52).

The resistance of *L. lactis* IL-1403 bacteria to c2 phage infection was confirmed by the lack of lytic activity of the phage with both free cells and biofilms. At the same time, fluctuations of the fluorescence intensity of labeled phage were detected throughout the thickness of the biofilm, although they could not be correlated over time. In view of this, we concluded that despite the resistance of *L. lactis* strain IL-1403 to c2 infection, initial phage binding to the cell surface was preserved, while the subsequent stage of phage development was blocked. A similar observation was reported for other c2-like bacteriophages (43). This result can be explained by the mechanisms of host cell infection by such phages. In *Lactococcus* gram-positive bacteria, the recognition receptors responsible for the initial phage-bacterium interactions are generally carbohydrates (rhamnose, glucose, galactose, etc.) exposed to the cell surface (54). In the case of c2-like prolate phage infection, a subsequent interaction occurs via PIP, a plasma membrane-associated protein required for the ejection of phage DNA (22, 36, 37). It was hypothesized that after the ejection of c2 phage DNA inside the host cell, phage development in *L. lactis* IL-1403 bacteria was blocked due to the action of an unidentified gene product encoded by one of the six prophages present in the IL-1403 genome (9; A. Aucouturier, personal communication).

Conclusions. Taken together, our experimental results demonstrate that bacteriophage in contact with a biofilm (i) could penetrate though the EPS matrix of the different biofilms studied and could also diffuse, as observed with the c2 phage in the insensitive *S. maltophilia* biofilms; (ii) could normally be immobilized, amplified, and released by a lytic cycle in the biofilm, as in the case of *L. lactis* OSM31 sensitive to the c2 bacteriophage; and (iii) could interact with their specific binding sites on the bacteria, even in the absence of lytic activity, as shown with the c2 phage in the nonpermissive strain *L. lactis* IL-1403. Thus, a natural ecosystem, such as a multispecies biofilm composed of phage-resistant and/or phage-sensitive strains, constitutes an "active" phage reservoir that not only can entrap and amplify viral particles and protect them from desiccation or sanitizing procedures but also allows phage dissemination for subsequent infection.

These results provide new perspectives that clarify our understanding of the persistence of lactococcal phages in dairy environments that preclude the activity of lactic acid bacteria.

ACKNOWLEDGMENTS

We thank the Essonne Département for financial support for the laser confocal microscope (grant ASTRE A02137).

We thank Victoria Hawken for correction of the English in the paper.

REFERENCES

1. **Atterbury, R. J., M. A. P. Van Bergen, F. Ortiz, M. A. Lovell, J. A. Harris, A. De Boer, J. A. Wagenaar, V. M. Allen, and P. A. Barrow.** 2007. Bacteriophage to reduce *Salmonella* colonization of broiler chickens. Appl. Environ. Microbiol. **73:**4543–4549.
2. **Banks, D. S., and C. Fradin.** 2005. Anomalous diffusion of proteins due to molecular crowding. Biophys. J. **89:**2960–2971.
3. **Bolotin, A., P. Wincker, S. Mauger, O. Jaillon, K. Malarme, J. Weissenbach, S. D. Ehrlich, and A. Sorokin.** 2001. The complete genome sequence of the lactic acid bacterium *Lactococcus lactis* IL1403. Genome Res. **11:**731–753.
4. **Brand, L., C. Eggeling, C. Zander, K. H. Drexhage, and C. A. M. Seidel.** 1997. Single molecule identification of coumarin 120 by time resolved fluorescence: comparison of one and two photon excitation in solution. J. Phys. Chem. **101:**4313–4323.
5. **Bren, L.** 2007. Bacteria eating virus approved as food additive. FDA Consumer. www.fda.gov/fdac/features/2007/107_virus.html.
6. **Brussaard, C. P. D.** 2004. Optimization of procedures for counting viruses by flow cytometry. Appl. Environ. Microbiol. **70:**1506–1513.
7. **Brüssow, H.** 2001. Phages of dairy bacteria. Annu. Rev. Microbiol. **55:**283–303.
8. **Casjens, S.** 2003. Prophages and bacterial genomics: what have we learned so far? Mol. Microbiol. **49:**277–300.
9. **Chopin, A., A. Bolotin, A. Sorokin, S. D. Ehrlich, and M. C. Chopin.** 2001. Analysis of six prophages in *Lactococcus lactis* IL1403: different genetic structure of temperate and virulent phage populations. Nucleic Acids Res. **29:**644–651.
10. **Christensen, B., C. Sternberg, J. B. Andersen, L. Eberl, S. Moller, M. Givskov, and S. Molin.** 1998. Establishment of new genetic traits in a microbial biofilm community. Appl. Environ. Microbiol. **64:**2247–2255.
11. **Clark, J. R., and J. B. March.** 2006. Bacteriophages and biotechnology: vaccines, gene therapy and antibacterials. Trends Biotechnol. **24:**212–218.
12. **Costerton, J. W., J. J. Cheng, G. G. Geesey, T. I. Ladd, J. C. Nickel, M. Dasgupta, and T. J. Marrie.** 1987. Bacterial biofilms in nature and disease. Annu. Rev. Microbiol. **41:**435–464.
13. **Costerton, J. W., P. S. Steward, and E. P. Greenberg.** 1999. Bacterial biofilms: a common cause of persistent infections. Science **284:**1318–1322.
14. **Curtin, J. J., and R. M. Donlan.** 2006. Using bacteriophages to reduce formation of catheter-associated biofilms by *Staphylococcus epidermidis*. Antimicrob. Agents Chemother. **50:**1268–1275.
15. **Davies, D., M. R. Parsek, J. P. Pearson, B. H. Iglewski, J. W. Costerton, and E. P. Greenberg.** 1998. The involvement of cell-to-cell signals in the development of a bacterial biofilm. Science **280:**295–298.
16. **Deveau, H., M. R. Van Calsteren, and S. Moineau.** 2002. Effect of exopolysaccharide on phage-host interactions in *Lactoccocus lactis*. Appl. Environ. Microbiol. **68:**4364–4369.
17. **Dobrindt, U., and J. Reidl.** 2000. Pathogenicity islands and phage conversion: evolutionary aspects of bacterial pathogenesis. Int. J. Med. Microbiol. **290:** 519–527.
18. **Doolittle, M. M., J. J. Cooney, and D. E. Caldwell.** 1995. Lytic infection of *Escherichia coli* biofilms by bacteriophage T4. Can. J. Microbiol. **41:**12–18.
19. **Elson, E. L., and D. Magde.** 1974. Fluorescence correlation spectroscopy: conceptual basis and theory. Biopolymers **13:**1–27.
20. **Emond, E., E. Dion, S. A. Walker, E. R. Vedamuthu, J. K. Kondo, and S. Moineau.** 1998. AbiQ, an abortive infection mechanism from *Lactococcus lactis*. Appl. Environ. Microbiol. **64:**4748–4756.
21. **Fischetti, V. A., D. Nelson, and R. Schuch.** 2006. Reinventing phage therapy: are the parts greater that the sum? Nat. Biotechnol. **24:**1508–1511.
22. **Geller, B. L., R. G. Ivey, J. E. Trempy, and B. Hettinger-Smith.** 1993. Cloning of a chromosomal gene required for phage infection of *Lactococcus lactis* subsp. *lactis* C2. J. Bacteriol. **175:**5510–5519.
23. **Guiot, E., M. Enescu, B. Arrio, G. Johannin, G. Roger, S. Tosti, F. Tfibel, M. Mérola, A. Brun, P. Georges, and M. P. Fontaine-Aupart.** 2000. Molecular dynamics of biological probes by fluorescence correlation microscopy with two photon excitation. J. Fluoresc. **10:**413–419.
24. **Guiot, E., P. Georges, A. Brun, M. P. Fontaine-Aupart, M. N. Bellon-Fontaine, and R. Briandet.** 2002. Heterogeneity of diffusion inside microbial biofilms determined by fluorescence correlation spectroscopy under two-photon excitation. Photochem. Photobiol. **75:**570–578.
25. **Hanlon, G. W., S. P. Denyer, C. J. Olliff, and L. J. Ibrahim.** 2001. Reduction in exopolysaccharide viscosity as an aid to bacteriophage penetration through *Pseudomonas aeruginosa* biofilms, Appl. Environ. Microbiol. **67:** 2746–2753.
26. **Hudson, J. A., C. Billington, G. Carey-Smith, and G. Greening.** 2005. Bacteriophages as biocontrol agents in food. J. Food Prot. **68:**426–437.
27. **Hughes, K. A., I. W. Sutherland, J. Clarks, and M. V. Jones.** 1998. Bacteriophage and associated polysaccaride depolymerases—novel tools for study of bacterial biofilms. J. Appl. Microbiol. **85:**583–590.
28. **Hughes, K. A., I. W. Sutherland, and M. V. Jones.** 1998. Biofilm susceptibility to bacteriophage attack: the role of phage-borne polysaccharide depolymerase. Microbiology **144:**3039–3047.
29. **Klausen, M., A. Aaes-Jorgensen, S. Molin, and T. Tolker-Nielsen.** 2003. Involvement of bacterial migration in the development of complex multicellular structures in *Pseudomonas aeruginosa* biofilms. Mol. Microbiol. **50:** 61–68.
30. **Lacroix-Gueu, P., R. Briandet, S. Lévêque-Fort, M. N. Bellon-Fontaine, and M. P. Fontaine-Aupart.** 2005. In situ measurements of viral particles diffusion inside mucoid biofilms. C. R. Biol. **328:**1065–1072.
31. **Lawrence, J. R., D. R. Korber, B. D. Hoyle, J. W. Costerton, and D. E. Caldwell.** 1991. Optical sectioning of microbial biofilms. J. Bacteriol. **173:** 6558–6567.
32. **Liu, J., M. Dehbi, G. Moeck, F. Arhin, P. Bauda, D. Bergeron, M. Callejo, V. Ferretti, N. Ha, T. Kwan, J. McCarty, R. Srikumar, D. Williams, J. J. Wu, P.**

Gros, J. Pelletier, and M. Dubow. 2004. Antimicrobial drug discovery through bacteriophages genomics. Nat. Biotechnol. **22:**185–191.
33. **Lu, K. T., and J. Collins.** 2007. Dispersing biofilms with engineered enzymatic bacteriophage. Proc. Natl. Acad. Sci. USA **104:**11197–11202.
34. **Lubbers, M. W., N. R. Waterfield, T. P. J. Beresford, R. W. F. Le Page, and A. W. Jarvis.** 1995. Sequencing and analysis of the prolate-headed lactococcal bacteriophage c2 genome and identification of the structural genes. Appl. Environ. Microbiol. **61:**4348–4356.
35. **Matsuzaki, S., M. Rashel, J. Uchiyamam, S. Sakurai, T. Ujihara, M. Kuroda, M. Ikeuchi, T. Tani, M. Fujieda, H. Wakiguchi, and S. Imai.** 2005. Bacteriophage therapy: a revitalized therapy against bacterial infectious diseases. J. Infect. Chemother. **11:**211–219.
36. **Monteville, M. R., B. Ardestani, and B. L. Geller.** 1994. Lactococcal bacteriophages require a host cell wall carbohydrate and a plasma membrane protein for adsorption and ejection of DNA. Appl. Environ. Microbiol. **60:**3204–3211.
37. **Mooney, D. T., M. Jann, and B. L. Geller.** 2006. Subcellular location of phage infection protein (Pip) in *Lactococcus lactis*. Can. J. Microbiol. **52:**664–672.
38. **Petersen, N., and E. Elson.** 1986. Measurements of diffusion and chemical kinetics by fluorescence photobleaching. Methods Enzymol. **130:**454–484.
39. **Petty, N. K., T. J. Evans, P. C. Fineran, and G. P. C. Salmond.** 2007. Biotechnological exploitation of bacteriophages research. Trends Biotechnol. **25:**7–15.
40. **Prigent, M., M. Leroy, F. Confalonieri, M. Dutertre, and M. S. Dubow.** 2005. A diversity of bacteriophage forms and genomes can be isolated from the surface sands of the Sahara Desert. Extremophiles **9:**289–296.
41. **Projan, S.** 2004. Phage inspired antibiotics? Nat. Biotechnol. **22:**167–168.
42. **Quignon, F., M. Sardin, L Kiene, and L. Schwartzbrod.** 1997. Poliovirus-1 inactivation and interaction with biofilm: a pilot-scale study. Appl. Environ. Microbiol. **63:**978–982.
43. **Rakonjac, J., P. W. O'Toole, and M. W. Lubbers.** 2005. Isolation of lactococcal prolate phage-phage recombinants by an enrichment strategy reveals two novel host range determinants. J. Bacteriol. **187:**3110–3121.
44. **Resch, A., B. Fehrenbacher, K. Eisele, M. Schaller, and F. Götz.** 2005. Phage release from biofilm and planktonic *Staphylococcus aureus* cells. FEMS Microbiol. Lett. **252:**89–96.
45. **Roth, B. L., M. Poot, S. T. Yue, and P. J. Millard.** 1997. Bacterial viability and antibiotic susceptibility testing with SYTOX green nucleic acid stain. Appl. Environ. Microbiol. **63:**2421–2431.
46. **Schwille, P., and E. Haustein.** 2001. Fluorescence correlation spectroscopy: an introduction to its concepts and applications, p. 1–33. *In* E. L. Elson and R. Rigler (ed.), Fluorescence correlation spectroscopy. Theory and applications. Springer, Berlin, Germany.
47. **Sillankorva, S., R. Oliveira, M. J. Vieira, I. W. Sutherland, and J. Azeredo.** 2004. Bacteriophage ϕS1 infection of *Pseudomonas fluorescens* planktonic cells versus biofilms. Biofouling **20:**133–138.
48. **Skurnik, M., and E. Strauch.** 2006. Phage therapy: facts and fiction. Int. J. Med. Microbiol. **296:**5–14.
49. **Stewart, P. S., and J. W. Costerton.** 2001. Antibiotic resistance of bacteria in biofilms. Lancet **358:**135–138.
50. **Storey, M. V., and N. J. Ashbolt.** 2003. Enteric virions and microbial biofilms—a second source of public health concern? Water Sci. Technol. **48:** 97–104.
51. **Sulakvelidze, A., Z. Alavidza, and J. G. Morris, Jr.** 2001. Bacteriophage therapy. Antimicrob. Agents Chemother. **45:**649–659.
52. **Suthereland, I. W., K. A. Hugues, L. C. Skillman, and K. Tait.** 2004. The interaction of phage and biofilms. FEMS Microbiol. Lett. **232:**1–6.
53. **Terzaghi, B. E., and W. E. Sandine.** 1975. Improved medium for lactic streptococci and their bacteriophages, Appl. Environ. Microbiol. **29:**807–813.
54. **Valyasevi, R., W. E. Sandine, and B. L. Geller.** 1991. A membrane protein is required for bacteriophage c2 infection of *Lactococcus lactis* subsp. *lactis* c2. J. Bacteriol. **173:**6095–6100.
55. **Wachsmuth, M., W. Waldeck, and J. Langowski.** 2000. Anomalous diffusion of fluorescent probes inside living cell nuclei investigated by spatially resolved fluorescence correlation spectroscopy. J. Mol. Biol. **298:**677–689.
56. **Webb, J. S., L. S. Thompson, S. James, T. Chartlton, T. Tolkier-Nielsen, B. Koch, M. Givskov, and S. Kjelleberg.** 2003. Cell death in *Pseudomonas aeruginosa* biofilm development. J. Bacteriol. **185:**4585–4592.
57. **Webb, J. S., M. Lau, and S. Kjelleberg.** 2004. Bacteriophage and phenotypic variation in *Pseudomonas aeruginosa* biofilm development, J. Bacteriol. **186:** 8066–8073.